High Vacuum Flat Plate Photovoltaic-Thermal (PV-T) Collectors: Efficiency Analysis

Daniela De Luca[a,c], Paolo Strazzullo[b,c], Emiliano Di Gennaro[a,c], Antonio Caldarelli[b,c], Eliana Gaudino[b,c], Marilena Musto[b,c], Roberto Russo[c]

[a] *Physics Department, University of Napoli "Federico II", Via Cinthia, 21, Napoli, 80126, Italy*
[b] *Industrial Engineering Department, University of Napoli "Federico II", Piazzale Vincenzo Tecchio, 80, Napoli, 80125, Italy*
[c] *Institute of Applied Sciences and Intelligent Systems, National Research Council of Italy, Via Pietro Castellino 111, Napoli, 80131, Italy*

Abstract

We investigate the performance of a novel flat photovoltaic-thermal (PV-T) module under high-vacuum through a 1D numerical model based on steady-state energy balance, with the aims of optimizing the simultaneous production of thermal and electrical energy. In the proposed design, the photovoltaic (PV) cell is positioned directly above the selective solar absorber (SSA), in a multilayer or fully integrated PV-SSA structure, which allows full exploitation of spectral solar radiation. In fact, in this configuration the losses related to non-absorption of low-energy photons and thermalization, typical of a classical single-junction PV cell, are reduced. The present study is conducted as the emittance and energy bandgap of the PV layer varied, thus admitting a wide variety of materials into the analysis. The dependence of the temperature coefficient, β (%/K), on the energy bandgap of the PV cell is also included. In the last part of the work, we discuss the performance of the proposed evacuated PV-T equipped with a SSA layer and thin film solar cells, namely those made of CdTe, CdS and GaAs. Overall, the paper highlights the great advantage of using high vacuum insulation, which suppresses conductive losses, and the versatility of the proposed system, which could be adapted to the user's needs simply by choosing the appropriate material for the photovoltaic layer.

Keywords: Solar energy, photovoltaic-thermal, electrical efficiency, thermal efficiency, exergetic efficiency, energy bandgap

1. Introduction

One of the most topical and interesting themes nowadays is undoubtedly climate change: according to the Global Risks Perception Survey (GRPS) of 2022 the *climate action failure* is perceived as the number one long-term global threat with the most severe impacts over the next decade [1]. Hence the race for renewable energies becomes fundamental: solar energy is the one that attracts the most interest as, despite about half of the solar radiation is either absorbed or reflected by the clouds and the atmosphere, the Earth's surface still receive enough power to meet the demands of the whole world [2, 3]. Once solar energy is harvested, it can be converted into electrical or thermal energy thanks to solar cells and solar thermal devices, respectively.

While solar thermal systems can boast high conversion efficiencies, up to 80%, solar cells are able to convert only a small percentage of the received solar radiation into electricity: according to the theoretical study made by W. Shockley and H.J. Queisser [4], which defines an ideal situation with specific assumptions [5], with a single p-n junction operating at room temperature under an AM 1.5 solar spectrum, the maximum solar-to-electrical energy conversion efficiency achievable is of 33.7% if one use a cell with bandgap of 1.4 eV. Lower efficiencies are obtained in reality, due to non-ideal absorption, non-radiative recombination, etc [5, 6]. Indeed the highest value recorded is of (29.1 ± 0.6)% for single-junction cells made of GaAs [7, 8]. The remaining fraction of solar radiation hitting the PV cell is either not absorbed or wasted as heat [9]. To avoid this, new systems consisting of a combination of a solar cell and a thermal collector are gaining interest. Not only are these *photovoltaic-thermal* (PV-T) devices capable of exploiting more solar radiation than a typical PV module, but they also allow for a) the simultaneous production of thermal and electrical energy [10], thus enabling to also cover energy demands of heat (which globally accounts for nearly the 50% of energy needs) and b) the maximization of energy yield per unit of space [11, 12].

Preprints (www.preprints.org) | NOT PEER-REVIEWED | Posted: 30 November 2022 doi:10.20944/preprints202211.0571.v1

The idea of PV-T systems originated in the 1970s [13, 14, 15]; since then efforts have been made to design a device that could provide good performance combined with low cost. Several works have modeled and predicted the performance of PV-Ts, which can exist in a flat-plate or concentrating layout. Since concentrating collectors require reflectors, lenses, and a sunlight tracking mechanism that make the overall system expensive and complex, except for the industrial applications, the flat-plate layout is preferred.
So far, most of the developed flat PV-T systems were able to provide low temperature heat (water heated at $\simeq$ 30-40 $^\circ$ C), reducing the number of installations as only a few end use demands could have been met. Increasing such temperature could guarantee a higher installation rate but, unfortunately, both thermal and electrical efficiencies decrease with the operating temperature.

On the electrical side, the solar-to-electrical energy conversion efficiency (η_{el}) drops dramatically with temperature, according to the following equation [16, 17]:

$$\eta_{el} = \eta_0[1 + \beta(E_{bg}, T_{PV}) \cdot (T_{PV} - T_{NOCT})], \tag{1}$$

where η_0 is the electrical efficiency calculated at the Nominal Operating Cell Temperature (NOCT), approximately 50 °C; T_{PV} is the operating temperature of the PV cell and $\beta(E_{bg}, T_{PV})$ <0 is the temperature coefficient of the PV module, indicating that the electrical efficiency is affected not only by temperature but also by the bandgap energy of the photovoltaic material. This will be better highlighted in Section 2.1. Notwithstanding that, there are many cases in which PV modules undergo high-illumination and high-temperature conditions (> 150 °C), such as in long-duration space missions. In fact, solar cells and solar arrays [18] are, among other options, the only systems currently capable of providing stable and uninterrupted electrical power [19]. Therefore, both the performance of wide-bandgap materials - such as GaP, SiC, GaN [20], GaAs [21, 22] - and of multi-junction solar cells [23, 24] have been investigated for use in high-temperature environments. More recent studies have also highlighted the advantages of developing perovskite solar cells for space technology applications [25, 26].

On the thermal side, the reduction of the solar-to-thermal energy conversion efficiency (η_{th}) is mainly due to radiative and convective losses. The latter could be easily reduced if one uses a high-vacuum insulation: high vacuum flat thermal panels are already available on the market [27] and show impressive performance compared to the traditional ones [28]. In this context, recent works have already proposed the idea of evacuated PV-T systems: Mellor et al. [29] have demonstrated the enormous advantages of such a system, which can double the thermal efficiency; Hu et al. [30] have shown that the vacuum encapsulation allows to enhance the total efficiency by nearly 10% at temperature higher than 80 °C. However, they based their analysis on PV cell laminated on the metal sheet using polymeric/organic foils aiming at the maximization of electrical efficiency by considering the heat produced at low temperatures as an additional product of the process.

In a recent article by De Luca et al. [31][1], the authors proposed two novel layouts of evacuated hybrid PV-T collectors that faithfully reproduce the existing high-vacuum flat plate (HVFP) collector produced by TVP Solar [27]: an evacuated metallic case is covered by a highly transparent glass and is equipped with a selective solar absorber (SSA). Of course, the systems also include a PV layer, which in principle could be placed below the glass cover (layout **A**) or above the SSA (layout **B**). The goal is year-round heat generation at medium temperatures, where the main technological challenges lie, and efficient power generation.
However, in [31] we demonstrated that layout **B**, rather than layout **A**, is the one that maximizes the conversion of solar energy to electrical+thermal energy, allowing the entire portion of the solar spectrum not converted to electricity by the PV layer to reach the SSA below (see in particular Figs. 1 and 7 in [31]). However, the previous model was developed by setting β=-0.2 %/K, limiting the description to a few real solar cells (mainly crystalline silicon cells). Thus, in this work we overcome this limitation by also including the temperature coefficient dependence on the bandgap energy. Then, we evaluate the thermal, electrical, total and exergetic efficiencies of the system, whose design is schematically illustrated in Fig. 1. We finally included calculations based on different PV cells thin film materials and on experimental data on real cells.
The article is divided in two main sections: Section 2 describes the technique used for simulating the performance of an evacuated flat PV-T collector; Section 3 illustrates the key findings of the efficiency analysis and reports some results obtained with experimental data from literature. Finally, we conclude the work by summarizing the findings and proposing new perspectives (Section 4).

[1] Soon available in Energy Reports

Preprints (www.preprints.org) | NOT PEER-REVIEWED | Posted: 30 November 2022 doi:10.20944/preprints202211.0571.v1

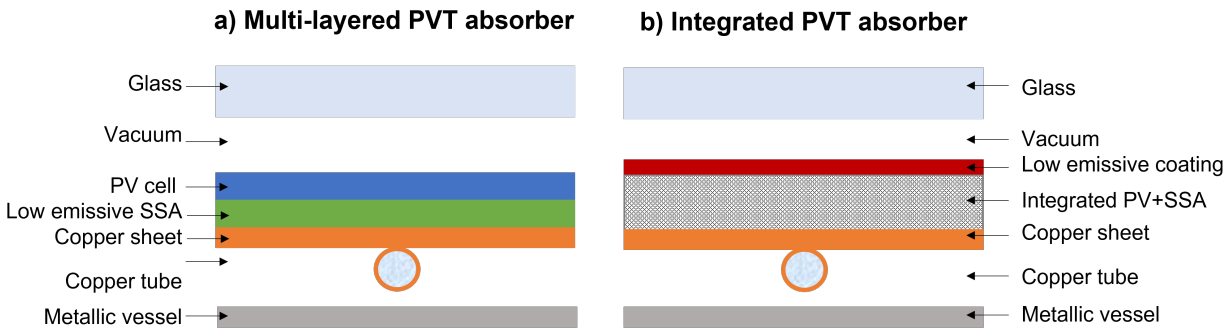

Figure 1: Cross-section schematics of the evacuated PV-T architecture proposed: the PV cell could either be a) fabricated on top of the absorber to form a multi-layered PVT absorber or b) fully-integrated in a PV-SSA layer.

2. Methods

In Section 2.1 we show the temperature coefficient dependence on PV module temperature, T_{PV}, and bandgap energy, E_{bg}; then we describe the physical model of the evacuated PV-T system (in Section 2.2), and list the various efficiency components useful to evaluate the performance of the proposed system (Section 2.3).

2.1. Temperature coefficient (β) dependence on PV module temperature and bandgap energy

The β(%/K) coefficient is expressed as the percentage decrease in output for each degree of the PV cell operating temperature increase, starting from T_0=300 K. Its variation with the cell bandgap can be evaluated from the Shockley-Queisser (SQ) limit (η_{SQ}) at a certain E_{bg}, and calculated both at the operating temperature of T_0=300 K and at a generic T_{PV} ($T_{PV}\neq$300 K) of interest. After doing some math we arrive at the following equation for $\beta = \beta(E_{bg}, T_{PV})$:

$$\beta(E_{bg}, T_{PV}) = \left(\frac{\eta_{SQ}(E_{bg}, T_{PV})}{\eta_{SQ}(E_{bg}, T_0)} - 1 \right) \cdot \frac{1}{T_{PV} - T_0}. \tag{2}$$

Eq. 2 has been included in the efficiency calculations.

2.2. Physical model of evacuated PV-T system

The HVFP collector produced by TVP Solar has dimensions of 1 m x 2 m wide. Since it has a thickness of about 0.05 m (thus much thinner than the lateral dimensions), we can use the infinite-layer approximation, already validated in previous works [32, 33]. Hence, the evacuated PV-T device is modeled by using a 1D thermal model developed in MATLAB and based on the steady-state balance of energy on its main components (glass cover and PV-SSA layer). Note that the study has been performed by assuming the SQ ideal limit for the estimation of the PV cell efficiency. Concerning the calculation of the thermal efficiency, realistic values of absorptance in the solar region and emittance have been selected for the SSA, i.e. α_{SSA}=0.95 in the solar spectral region and ε_{SSA}=0.05 elsewhere, according to previous literature [33].

Glass cover. It considers the convective losses to the ambient and the radiative exchange toward the PV layer:

$$I \cdot \alpha_{gl} + h_w \cdot (T_{amb} - T_{gl}) + \varepsilon_{gl-PV} \cdot \sigma \cdot (T_{PV}^4 - T_{gl}^4) = 0, \tag{3}$$

where I=$\int_0^\infty S(\lambda)\, d\lambda$ is the integral of the solar radiation spectral distribution $S(\lambda)$, α_{gl}=0.95 is the glass absorptance, h_w is the heat convection coefficient ($h_w = 4.5 + 2.9\ u_w$, where u_w <5 m/s is the wind speed), ε_{gl-PV} is the equivalent emissivity of glass-PV, and σ is the Stephan-Boltzmann constant.

PV-SSA layer. It considers the radiative loss to glass and vessel, in addition to the radiation converted in electrical and thermal power:

$$I' - \sigma \cdot [\varepsilon_{gl-PV} \cdot (T_{PV}^4 - T_{gl}^4) - \varepsilon_{SSA-ves} \cdot (T_{SSA}^4 - T_{ves}^4)] - P_{el} - P_{th} = 0 \tag{4}$$

Preprints (www.preprints.org) | NOT PEER-REVIEWED | Posted: 30 November 2022 doi:10.20944/preprints202211.0571.v1

where $I'=I \cdot \tau_{gl} \cdot \alpha_{PV-T}$, $\varepsilon_{SSA-ves}$ is the equivalent emissivity of the SSA facing the vessel, P_{el} and P_{th} indicates the produced electrical and thermal power, respectively.

2.3. PV-T performance evaluation

The performance of the evacuated PV-T system is evaluated in terms of electrical, thermal, total and exergy efficiencies of the system. The **electrical efficiency** is calculated according to Eq. 1, while thermal, total, and exergetic efficiency are defined by Eqs. 5-7:

- thermal efficiency

$$\eta_{th} = \frac{P_{th}}{I}, \tag{5}$$

- total efficiency

$$\eta_{tot} = \eta_{th} + \eta_{el}, \tag{6}$$

- exergetic efficiency

$$\eta_{ex} = \frac{P_{el} + P_{th} \cdot \eta_C}{(1 - \frac{T_{amb}}{T_{Sun}}) \cdot I}, \tag{7}$$

where η_C indicates the Carnot efficiency, $\eta_C = 1 - T_{amb}/T_{SSA}$.

3. Results

In the following, we present the main results of the analysis performed on the temperature coefficient β (Section 3.1), and on the performance of the proposed PV-T system (Section 3.2). Furthermore, we discuss the results concerning realistic PV layers of GaAs, CdS and CdTe (Section 3.3).

3.1. Temperature coefficient $\beta = \beta(E_{bg}, T_{PV})$: results

The results of the study on the temperature coefficient dependence on the PV cell temperature and bandgap energy, calculated according Eq. 2, are showed in Fig. 2. Figure 2 (a) highlights that the value of β significantly depends on the energy bandgap, whereas the Fig. 2 (b) shows the SQ limit of the electrical efficiency for different operating temperatures of the PV module. It demonstrates that the choice of the optimal bandgap depends on the operating temperature, especially for low-to-medium bandgap energy values. For instance, materials with energy bandgap above 2.0 eV have a theoretical efficiency less dependent on the temperature.

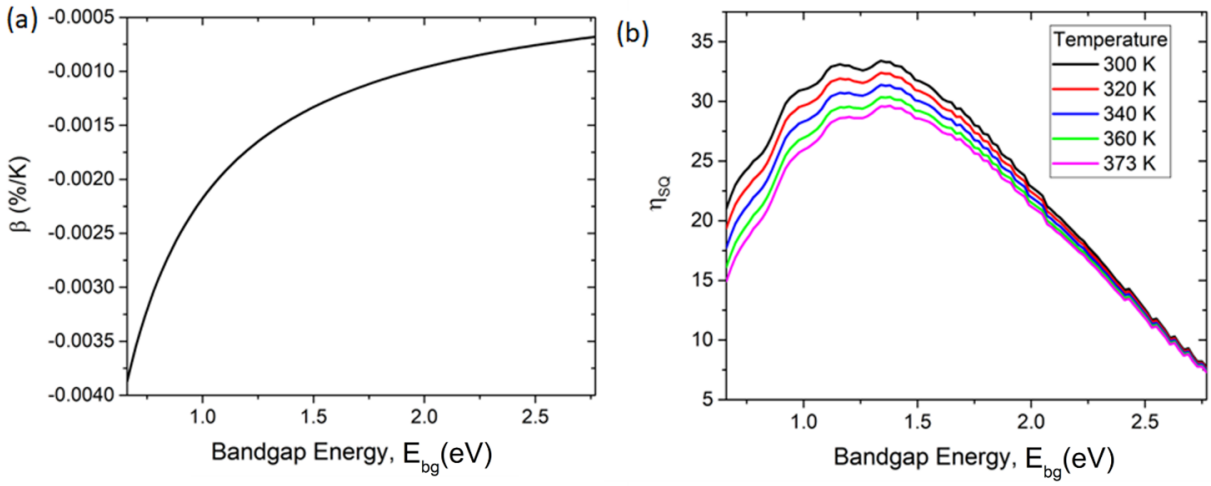

Figure 2: (a) Temperature coefficient dependence on the PV cell bandgap energy, E_{bg}, and temperature. (b) SQ limit of electrical efficiency for different PV module operating temperatures.

Preprints (www.preprints.org) | NOT PEER-REVIEWED | Posted: 30 November 2022 doi:10.20944/preprints202211.0571.v1

The validity of Eq. 2 was verified by comparing the results showed in Fig. 2 with those of a prior work by Vaillon et al. [6], where β is evaluated by the hypothesis of detailed balance [5]. The two models of β agree in the whole range of E_{bg} investigated.

3.2. PV-T performance evaluation vs energy bandgap and thermal emittance: results

The results of the analysis conducted on the PV-T system efficiency are depicted in Fig. 3, where colormaps of thermal, electrical, total and exergetic efficiency are shown as function of the PV layer emissivity, ε_{PV}, which varies in the range of 0 to 1, and of bandgap energy, E_{bg}, in [0.66; 2.70] eV. Each row refers to a different solar-to-X energy conversion efficiency (thermal: top row; electric: second row; total: third row; exergetic: bottom row), whereas the columns show the results of the calculation performed at different operating temperatures, from 323 K to 423 K. The thermal efficiency of the proposed PV-T system appears to be strongly dependent on the emissivity of the PV layer, especially when working at high temperatures. In contrast, the electrical efficiency results independent on ε_{PV}. In this case, as expected, the lower the temperature, the better the performance. Moreover, higher values of electrical efficiency are obtained by using photovoltaic cells with bandgap energy in the range of about 1.1 to 1.5 eV. At T=323 K, total efficiency is greater than 85% for any value of ε_{PV} and E_{bg} but, as temperature increases, a decrease in its value is observed, especially as ε_{PV} increases: the total efficiency reaches minimum values at high operating temperatures (T=423 K) and high values of ε_{PV} and E_{bg}. However, once the quality of heat produced is taken into account, it becomes clear that very interesting exergy results can be obtained if very low cell emittance values are used and that maximum exergy is obtained for a PV cell with a bandgap of about 1.4 eV.

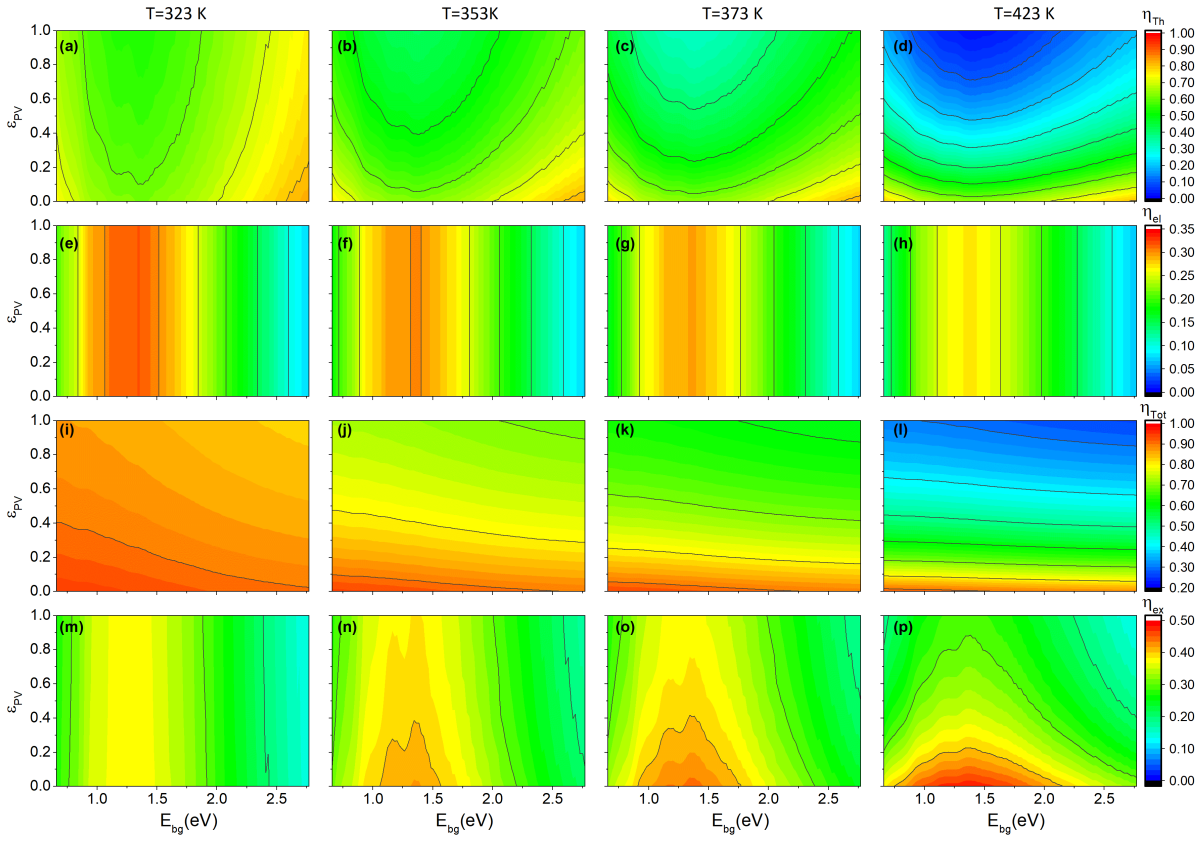

Figure 3: Thermal (a-d), electrical (e-h), total (i-l), and exergetic (m-p) efficiencies of an evacuated PV-T collector working at different temperatures in the range of 323 K (left column) to 423 K (right column). The various quantities are showed as function of the PV layer emissivity, ε_{PV}, and bandgap energy, E_{bg}.

Preprints (www.preprints.org) | NOT PEER-REVIEWED | Posted: 30 November 2022 doi:10.20944/preprints202211.0571.v1

3.3. PV-T performance evaluation for existing thin film solar cells

Although crystalline silicon is the most widely used material in PV applications, it is not suitable for PV-T applications where high operating temperatures of up to 150°C are required. To adopt a more genuine approach to hybrid PV-T cells, PV materials in form of thin film should be preferred.

Other semiconductor materials have emerged as thin films: amorphous silicon (a-Si), germanium (Ge), copper indium gallium diselenide (CIGS), cadmium sulfide (CdS), cadmium telluride (CdTe), gallium arsenide (GaAs), indium phosphide (InP), gallium indium phosphide (GaInP), and so on [34, 35].

Theoretical and experimental studies on the temperature dependence of various solar cells performance are reported in the literature. In [21] the authors explore the temperature dependence of the electrical properties of GaAs single-junction solar cells up to about 350 °C, showing a reduction in efficiency from ≃18% at 25 °C to 0% at 300-350 °C. A theoretical investigation of CdTe, InP, CdS, Si, Ge, and GaAs cells is reported in [36]; while [37] explores the case of (Al)GaInP/GaAs tandem solar cells.

Here, we want to evaluate the use of these cells in evacuated PV-T systems, and how the choice of material from which the photovoltaic layer is made can result in less or more electrical (and thus, oppositely, thermal) energy production at various temperatures. Three materials for the photovoltaic layer were examined: CdTe, CdS and GaAs. Theoretical data on the electrical efficiency were taken from [36]. The results of this analysis performed at four different temperatures (323, 353, 373 and 423 K) are shown in Fig. 4.

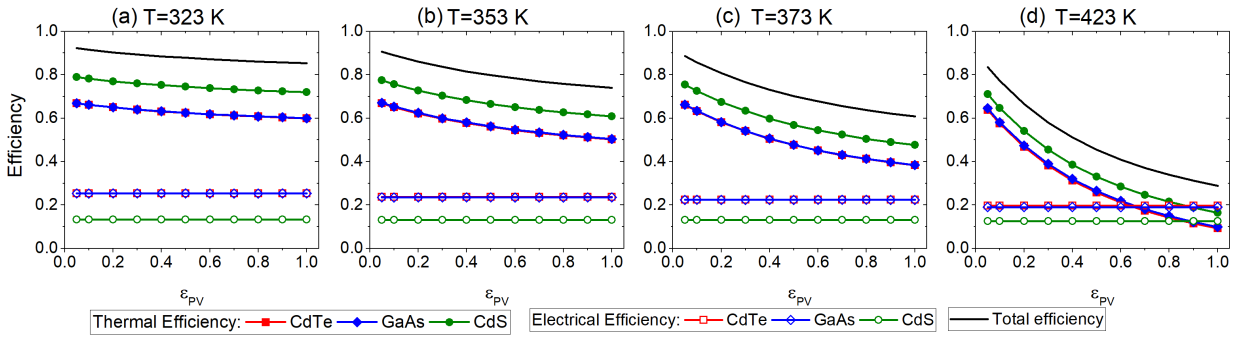

Figure 4: Thermal (filled symbols), electrical (empty symbols), and total (black continuous line) efficiency of an evacuated PV-T system equipped with a PV layer made of CdTe (red), GaAs (blue), or CdS (green lines and symbols), calculated at various temperatures: (a) 323 K, (b) 353 K, (c) 373 K, and (d) 423 K.

We observe that GaAs and CdTe cells perform very similarly, with thermal efficiencies above 60% for low values of emissivity, i.e. $\varepsilon_{PV} \leq 0.1$, and for each temperature examined. Instead, CdS cells provide an electrical efficiency lower than that produced in GaAs and CdTe cells, i.e. ≃ 14% vs. ≃ 25%. However, such low electrical energy corresponds to a higher thermal conversion efficiency, of about 70-80% at low ε_{PV}.

As already mentioned, real PV cells fail to actually work under the SQ assumptions, and their SQ efficiency values represent only an ideal limit. Figure 5 compares the theoretical and experimental performance of a GaAs cells in a temperature range of 323 K to 423 K. As might be expected, the experimental evaluation by Maros et al. [21] shows an electrical efficiency lower than the theoretical counterpart (by [36]) at each of the temperatures investigated, implying on the other hand a higher thermal efficiency. For instance, at a medium operating temperature of 373 K, if a low emissivity (i.e. ≤ 0.21 as reported by [38]) can be guaranteed[2], the electrical efficiency only reaches ≃ 16%, rather than the ≃ 22% expected from the theoretical study, and it is accompanied by a thermal energy production of ≃ 67%, instead of ≃ 60% at 373K. Similar experimental results can be expected in the case of PV cells based on CdTe thin films.

[2]Emissivity values lower than 0.2 can be achieved by using appropriately developed transparent conductive oxide (TCO) films

Preprints (www.preprints.org) | NOT PEER-REVIEWED | Posted: 30 November 2022 doi:10.20944/preprints202211.0571.v1

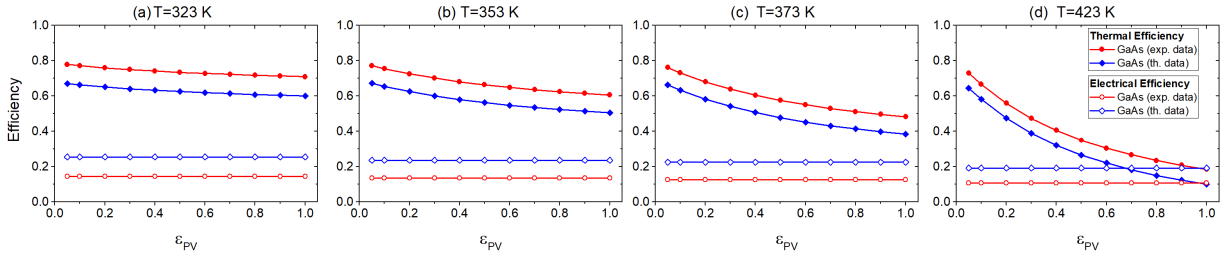

Figure 5: Thermal (filled symbols) and electrical (empty symbols) efficiency of the evacuated PV-T system equipped with a GaAs PV layer at (a) 323 K, (b) 353 K, (c) 373 K, and (d) 423 K. The red lines and symbols indicate the efficiency calculated according to the experimental data of the GaAs PV layer [21], the red lines and symbols refers to the theoretical data by [36].

4. Conclusions

In this work we considered the problem of maximizing the simultaneous production of thermal and electrical energy in evacuated flat plate photovoltaic-thermal (PV-T) collectors. The concept we investigated was to coat a PV layer on the selective solar absorber (SSA), in order to allow the entire portion of the solar spectral radiation not useful for electrical conversion to reach the SSA and be converted into thermal energy. We modeled the system by using a 1D thermal model based on the steady-state energy balance equations applied to the glass encapsulating the evacuated system and the couple PV-SSA layer. The amount of electrical and thermal efficiency obtainable from the proposed system was investigated at different operating temperatures, in the range of 323 K to 423 K, and at different value of thermal emittance of the PV-T cell structure. Overall, the study demonstrates that the system can be easily adapted to the customer's need: low operating temperatures and medium bandgap energies promote a production of electricity greater than that obtainable at higher temperatures, where also the thermal efficiency experiences a reduction due to the radiative losses towards the vessel. However, the low emissivity of the PV cell is the discriminating factor in achieving high thermal efficiency, particularly at medium-high temperatures.
PV cell based on CdS, CdTe, and GaAs were also investigated, indicating the possibility of obtaining good thermal and electrical efficiencies at low and medium operating temperatures. In a future perspective, a multi-junction photovoltaic cell could also be used: this would improve electrical performance at the expense of the thermal one.
In conclusion, the ability to fully exploit the solar spectrum and high-vacuum insulation enable promising results that require urgent experimental verification: the development of collectors based on such devices could lead us toward a cleaner, decarbonized world.

References

[1] The Global Risks Report 2022 - 17th edition, www3.weforum.org/docs/WEF_The_Global_Risks_Report_2022.pdf.
[2] C. Lauterbach, B. Schmitt, U. Jordan, K. Vajen, The potential of solar heat for industrial processes in Germany, Renewable and Sustainable Energy Reviews 16 (2012) 5121–5130. doi:10.1016/j.rser.2012.04.032.
[3] A. Shahsavari, M. Akbari, Potential of solar energy in developing countries for reducing energy-related emissions, Renewable and Sustainable Energy Reviews 90 (2018) 275–291. doi:10.1016/j.rser.2018.03.065.
[4] W. Shockley, H. J. Queisser, Detailed balance limit of efficiency of p-n junction solar cells, Journal of Applied Physics 32 (1961) 510–519.
[5] J.-F. Guillemoles, T. Kirchartz, D. Cahen, U. Rau, Guide for the perplexed to the shockley–queisser model for solar cells, Nature Photonics 13 (2019) 501–505. doi:10.1038/s41566-019-0479-2.
[6] R. Vaillon, S. Parola, C. Lamnatou, D. Chemisana, Solar cells operating under thermal stress, Cell Reports Physical Science 1 (2020) 100267. doi:10.1016/j.xcrp.2020.100267.
[7] M. Green, E. Dunlop, J. Hohl-Ebinger, M. Yoshita, N. Kopidakis, X. Hao, Solar cell efficiency tables (version 57), Progress in Photovoltaics: Research and Applications 29 (1) 3–15. doi:10.1002/pip.3371.
[8] B. M. Kayes, H. Nie, R. Twist, S. G. Spruytte, F. Reinhardt, I. C. Kizilyalli, G. S. Higashi, 27.6% conversion efficiency, a new record for single-junction solar cells under 1 sun illumination, 2011 37th IEEE Photovoltaic Specialists Conference (2011) 000004–000008.
[9] H. Teo, P. Lee, M. Hawlader, An active cooling system for photovoltaic modules, Applied Energy 90 (2012) 309–315. doi:10.1016/j.apenergy.2011.01.017.
[10] H. Zondag, Flat-plate PV-Thermal collectors and systems: A review, Renewable and Sustainable Energy Reviews 12 (2008) 891–959. doi:10.1016/j.rser.2005.12.012.
[11] M. Herrando, C. N. Markides, K. Hellgardt, A UK-based assessment of hybrid PV and solar-thermal systems for domestic heating and power: System performance, Applied Energy 122 (2014) 288–309. doi:10.1016/j.apenergy.2014.01.061.

[12] M. Farshchimonfared, J. Bilbao, A. Sproul, Channel depth, air mass flow rate and air distribution duct diameter optimization of photovoltaic thermal (PV/T) air collectors linked to residential buildings, Renewable Energy 76 (2015) 27–35. doi:10.1016/j.renene.2014.10.044.
[13] M. Wolf, Performance analyses of combined heating and photovoltaic power systems for residences, Energy Conversion 16 (1976) 79–90. doi:10.1016/0013-7480(76)90018-8.
[14] L. Florschuetz, Extension of the Hottel-Whillier model to the analysis of combined photovoltaic/thermal flat plate collectors, Solar Energy 22 (1979) 361–366. doi:10.1016/0038-092X(79)90190-7.
[15] S. D. Hendrie, Photovoltaic/thermal collector development program. final report (1982). doi:10.2172/5358100.
[16] S. Dubey, J. N. Sarvaiya, B. Seshadri, Temperature dependent photovoltaic (PV) efficiency and its effect on PV production in the world – a review, Energy Procedia 33 (2013) 311–321. doi:10.1016/j.egypro.2013.05.072.
[17] O. Dupré, R. Vaillon, M. Green, Physics of the temperature coefficients of solar cells, Solar Energy Materials and Solar Cells 140 (2015) 92–100. doi:10.1016/j.solmat.2015.03.025.
[18] International Space Station, nasa.gov/mission_pages/station/structure/elements/solar_arrays-about.html.
[19] A. Datas, A. Martí, Thermophotovoltaic energy in space applications: Review and future potential, Solar Energy Materials and Solar Cells (2017) 285–296doi:10.1016/j.solmat.2016.12.007.
[20] D. Merritt, S. Houlihan, R. P. Raffaelle, G. A. Landis, Wide-bandgap space solar cells, Conference Record of the Thirty-first IEEE Photovoltaic Specialists Conference, 2005 (2005) 552–555doi:10.1109/PVSC.2005.1488190.
[21] A. Maros, S. Gangam, Y. Fang, J. Smith, D. Vasileska, S. Goodnick, M. I. Bertoni, C. B. Honsberg, High temperature characterization of GaAs single junction solar cells, in: 2015 IEEE 42nd Photovoltaic Specialist Conference (PVSC), 2015, pp. 1–5. doi:10.1109/PVSC.2015.7356338.
[22] Y. Sun, J. Faucher, D. Jung, M. Vaisman, C. McPheeters, P. Sharps, E. Perl, J. Simon, M. Steiner, D. Friedman, M. L. Lee, Thermal stability of GaAs solar cells for high temperature applications, in: 2016 IEEE 43rd Photovoltaic Specialists Conference (PVSC), 2016, pp. 2385–2388. doi:10.1109/PVSC.2016.7750068.
[23] J. Grandidier, A. P. Kirk, M. L. Osowski, P. K. Gogna, S. Fan, M. L. Lee, M. A. Stevens, P. Jahelka, G. Tagliabue, H. A. Atwater, J. A. Cutts, Low-Intensity High-Temperature (liht) Solar Cells for Venus Atmosphere, IEEE Journal of Photovoltaics 8 (6) (2018) 1621–1626. doi:10.1109/JPHOTOV.2018.2871333.
[24] E. E. Perl, J. Simon, D. J. Friedman, N. Jain, P. Sharps, C. McPheeters, Y. Sun, M. L. Lee, M. A. Steiner, (Al)GaInP/GaAs tandem solar cells for power conversion at elevated temperature and high concentration, IEEE Journal of Photovoltaics 8 (2) (2018) 640–645. doi:10.1109/JPHOTOV.2017.2783853.
[25] V. Romano, A. Agresti, R. Verduci, G. D'Angelo, Advances in perovskites for photovoltaic applications in space, ACS Energy Letters 7 (8) (2022) 2490–2514. doi:10.1021/acsenergylett.2c01099.
[26] M. T. Hoang, Y. Yang, B. Tuten, H. Wang, Are metal halide perovskite solar cells ready for space applications?, The Journal of Physical Chemistry Letters 13 (13) (2022) 2908–2920. doi:10.1021/acs.jpclett.2c00386.
[27] TVPSolar, https://www.tvpsolar.com/.
[28] A. Buonomano, F. Calise, M. D. d'Accadia, G. Ferruzzi, S. Frascogna, A. Palombo, R. Russo, M. Scarpellino, Experimental analysis and dynamic simulation of a novel high-temperature solar cooling system, Energy Conversion and Management 109 (2018) 19–39.
[29] A. Mellor, D. A. Alvarez, I. Guarracino, A. Ramos, A. R. Lacasta, L. F. Llin, A. Murrell, D. Paul, D. Chemisana, C. Markides, N. Ekins-Daukes, Roadmap for the next-generation of hybrid photovoltaic-thermal solar energy collectors, Solar Energy 174 (2018) 386–398. doi:10.1016/j.solener.2018.09.004.
[30] M. Hu, C. Guo, B. Zhao, X. Ao, Suhendri, J. Cao, Q. Wang, S. Riffat, Y. Su, G. Pei, A parametric study on the performance characteristics of an evacuated flat-plate photovoltaic/thermal (PV/T) collector, Renewable Energy 167 (2021) 884–898. doi:10.1016/j.renene.2020.12.008.
[31] D. De Luca, A. Caldarelli, E. Gaudino, E. Di Gennaro, M. M., R. Russo, Modeling of energy and exergy efficiencies in high vacuum flat plate photovoltaic thermal (pv-t) collectors, Preprints 2022050355 (2022). doi:10.20944/preprints202205.0355.v1.
[32] C. D'Alessandro, D. D. Maio, M. Musto, D. D. Luca, E. D. Gennaro, P. Bermel, R. Russo, Performance analysis of evacuated solar thermal panels with an infrared mirror, Applied Energy 288 (2021). doi:https://doi.org/10.1016/j.apenergy.2021.116603.
[33] D. D. Maio, C. D'Alessandro, A. Caldarelli, D. D. Luca, E. D. Gennaro, M. Casalino, M. Iodice, M. Gioffre, R. Russo, M. Musto, Multilayers for efficient thermal energy conversion in high vacuum flat solar thermal panels, Thin Solid Films 735 (2021) 138869. doi:10.1016/j.tsf.2021.138869.
[34] B. Sopori, Thin-Film Silicon Solar Cells, John Wiley & Sons, Ltd, 2003, Ch. 8, pp. 307–357. doi:10.1002/0470014008.ch8.
[35] T. K. T. O. G. J. R. R. N. E. A. A. R. Jeyakumar Ramanujam, Douglas M. Bishop, Flexible cigs, cdte and a-si:h based thin film solar cells: A review, Progress in Materials Science 110 (2020) 100619. doi:10.1016/j.pmatsci.2019.100619.
[36] N. R. Priyanka Singh, Temperature dependence of solar cell performance—an analysis, Solar Energy Materials and Solar Cells 101 (2012) 36–45. doi:10.1016/j.solmat.2012.02.019.
[37] E. E. Perl, J. Simon, D. J. Friedman, N. Jain, P. Sharps, C. McPheeters, Y. Sun, M. L. Lee, M. A. Steiner, (al)GaInP/GaAs Tandem Solar Cells for Power Conversion at Elevated Temperature and High Concentration, IEEE Journal of Photovoltaics 8 (2) (2018) 640–645. doi:10.1109/JPHOTOV.2017.2783853.
[38] F. L. L. M. A. P. D. E.-D. N. Alonso-Álvarez, D., ITO and AZO films for low emissivity coatings in hybrid photovoltaic-thermal applications, Solar Energy 155 (2017) 82–92. doi:10.1016/j.solener.2017.06.033.